Acta Cryst. (1997). A**53**, 763–771

The Optical Activity of Crystalline L-Aspartic Acid

T. ASAHI, M. TAKAHASHI AND J. KOBAYASHI*

Kagami Memorial Laboratory for Material Science and Technology, Waseda University, 2-8-26 Nishi-Waseda, Shinjuku-ku, Tokyo 169, Japan

(Received 25 September 1996; accepted 21 March 1997)

Abstract

In a project of revealing gyro-optical properties of amino acids that build up proteins, all the components of the gyration tensor and the birefringence of L-aspartic acid have been successfully measured as a function of temperature although the crystal belongs to the monoclinic system. The temperature dependence of the rotation of the gyration surface around the crystallographic *b* axis was also clarified. It is of interest that the chirality index of this crystal was found to be almost the same as that of glutamic acid, another amino acid.

1. Introduction

Amino acids are important for generating the biological activity of proteins as their constituent units. It has been generally believed that the amino acids building up proteins are homochiral and L type. However, the direct optical confirmation of the chirality of any crystalline amino acids have not been made except for L,D-glutamic acids (Asahi, Utsumi, Itagaki, Kagomiya & Kobayashi, 1996). Asahi, Utsumi, Itagaki, Kagomiya & Kobayashi (1996) found that the two enantiomers of glutamic acid produce gyration-tensor components of the same magnitudes but of opposite signs. Comprehensive gyro-optical studies on amino acids are necessary for a deeper understanding of the biological functions of various proteins.

As a subsequent step of investigating the optical activity (OA) of crystalline amino acids, crystalline L-aspartic acid (AA) was studied. It has recently been clarified that L-AA plays an important role in proteins. For example, AA residues in αA- and αB-crystallin from human lens undergo simultaneous stereoinversion, isomerization and racemization during aging and cataract formation (Masters, Bada & Zigler, 1977; Fujii, Ishibashi, Satoh, Fujino & Harada, 1994; Fujii, Satoh, Harada & Ishibashi, 1994).

The crystal structure of L-AA was analyzed by Bernal (1931) by using X-rays. However, he overlooked a twinning mechanism by taking a unit cell twice the size of the true one. The correct structure was solved later by Derissen, Endeman & Peerdeman (1968), the space group being determined as monoclinic C_2^2-$P2_1$. Suresh & Vijayan (1983) reported that another form of L-AA was obtained accidentally during attempts to replace aspartic acid in L-ornithyl-L-aspartate by acetic acid. Its space group was orthorhombic D_2^4-$P2_12_12_1$.

Our specimens were monoclinic L-AA without twins. The indicatrix of the specimens should rotate spontaneously with change of temperature. For this reason, measurements of the optical properties of L-AA were anticipated to be very difficult. We applied the HAUP (high-accuracy universal polarimeter) (Kobayashi & Uesu, 1983; Kobayashi, Kumomi & Saito, 1986; Kobayashi, Asahi, Takahashi & Glazer, 1988) to this optically challenging crystal.

2. Optical nature

A plate crystal with dimensions of $5 \times 2 \times 0.8$ mm was grown from aqueous solution by slow evaporation at 303 K. It was vitreous in color. The lattice constants were measured by using Weissenberg photographs (*b*- and *c*-axis rotations): $a = 7.62$ (7.617), $b = 6.99$ (6.982), $c = 5.17$ Å (5.142 Å) and $\beta = 99.8°$ (99.84°) at 296 K. They coincided with the data reported by Derissen, Endeman & Peerdeman (1968) (given in parentheses). The extinction rule for $0k0$ reflections was consistent with that of C_2^2-$P2_1$. The absence of twinning in our specimens was also confirmed by microscopic, normal and conoscopic, observations.

The reference axes (x_1, x_2, x_3) were chosen as follows. As shown in Fig. 1, the x_2 axis was taken parallel to the monoclinic unique *b* axis following usual custom. The x_3 axis was adopted along the *c* axis. Therefore, the x_1 axis was parallel to the a^* axis, which was perpendicular to the (100) plane. Needless to say, the c^* axis was normal to the (001) plane.

The components of the gyration tensor referred to the reference axes are expressed by the matrix

$$\begin{bmatrix} g_{11} & 0 & g_{13} \\ & g_{22} & 0 \\ & & g_{33} \end{bmatrix}. \qquad (1)$$

In order to determine the four components of the gyration tensor, four different experiments were necessary. Define the wave normal of the incident light beam as $\mathbf{s}$ (s_1, s_2, s_3), where $s_1 = \cos\theta_1$,

$s_2 = \cos\theta_2$ and $s_3 = \cos\theta_3$ are direction cosines with the reference axes. We prepared four plate specimens numbered (i), (ii), (iii) and (iv); the major surfaces of each specimen being perpendicular to **s**(1,0,0), **s**(0,1,0), **s**(0,0,1) and **s**($\sin\theta$, 0, $\cos\theta$), respectively. Specimens (i) and (ii) were synonymous with (100) and (010) specimens. Specimen (iii) was prepared by polishing a (001) plate so as to become normal to the c axis. We took $\theta = -47.6°$ in specimen (iv). The method of the determination of θ will be explained later. Four gyrations, G_1, G_2, G_3 and G_4, obtained from the above specimens are expressed by the gyration-tensor components

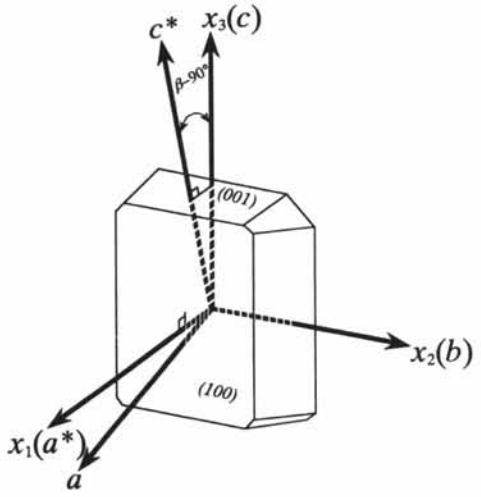

Fig. 1. Relationship between the reference axes (x_1, x_2, x_3) and the crystallographic axes (a, b, c).

$$G_1 = g_{11}, \quad G_2 = g_{22}, \quad G_3 = g_{33}$$

and

$$G_4 = g_{11}\sin^2\theta + g_{33}\cos^2\theta + 2g_{13}\sin\theta\cos\theta. \qquad (2)$$

In order to ensure the correct determination of the signs of the gyration-tensor components, the optical nature of L-AA was examined first. The principal axes of the indicatrix were defined as (X_1, X_2, X_3). As is usual, the X_2 axis coincides with the x_2 axis. Then, the X_1 and X_3 axes are contained in specimen (ii). Figs. 2(*a*), (*b*) and (*c*) show polarizing microscopic figures on specimen (ii). Fig. 2(*a*) indicates the conoscopic figure at an extinction position, where X_1 and X_3 axes were found to make angles of approximately 49 and $-41°$ with the x_3 axis, respectively. Fig. 2(*b*) shows the same figure at a diagonal position. The existence of the two melatopes showed that the (X_1, X_2) plane was the optic plane and the X_3 axis was optically the Y axis. Insertion of a $\lambda/4$ plate with the indicated orientation in Fig. 2(*c*) increased the path difference between the X_1 and X_3 axes of the specimen, manifesting that X_1 and X_3 axes were optically Z' and X' axes, respectively. Thus, it was determined that axes X_1, X_2 and X_3 were optically axes Z, X and Y. The optical orientation of L-AA is stereographically depicted in Fig. 2(*d*).

3. Measurement of optical properties

All the components of G and birefringence Δn of L-AA were measured by using HAUP. The specimens were put in a vacuum chamber and fixed at various temperatures between 380 and 200 K with an accuracy of ± 0.02 K. The light source was an He–Ne laser with a

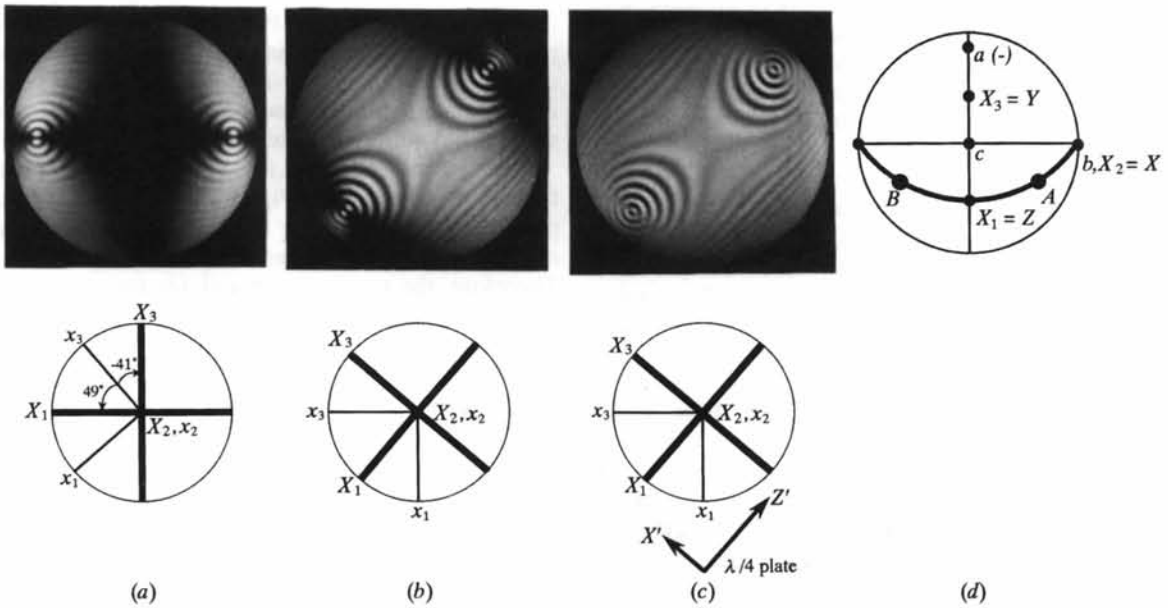

Fig. 2. Polarizing microscopic figures of specimen (ii) of L-AA: (*a*) at an extinction position; (*b*) at a diagonal position; (*c*) at the diagonal position when a $\lambda/4$ plate was inserted. (*d*) Stereographic projection of the optical orientation.

wavelength of 6328 Å. HAUP measurements provide us with the following three quantities:

$$\Delta = (2\pi d/\lambda)\Delta n, \tag{3}$$

$$B(0) = (\gamma - 2k)\sin\Delta + 2\delta\Upsilon\cos^2(\Delta/2) \tag{4}$$

or

$$B(0)/\sin\Delta = \gamma - 2k + \delta\Upsilon\cot(\Delta/2) \tag{5}$$

and

$$\theta_0 = -\tfrac{1}{2}(p+q)\cot(\Delta/2) - \tfrac{1}{2}\delta\Upsilon + \Psi, \tag{6}$$

where $\gamma = p - q$. d is the thickness of the specimen, k the ellipticity of the eigenpolarization in the crystal and Ψ the rotation angle of the indicatrix; p and q are systematic errors of parasitic ellipticities of the polarizer and analyzer and $\delta\Upsilon$ is the error of the deflecting angle of the analyzer from the crossed Nicols position. For all the specimens except (ii), (6) does not contain Ψ. In those cases, the systematic error γ could be simply determined by using the reference crystal method (Kobayashi, Asahi, Takahashi & Glazer, 1988). Moxon & Renshaw (1990) suggested another method for the determination of γ. On the other hand, $\delta\Upsilon$ could be obtained from $B(0)$ at special values of $\Delta = 2n\pi$ (n: integer). After these systematic errors were determined,

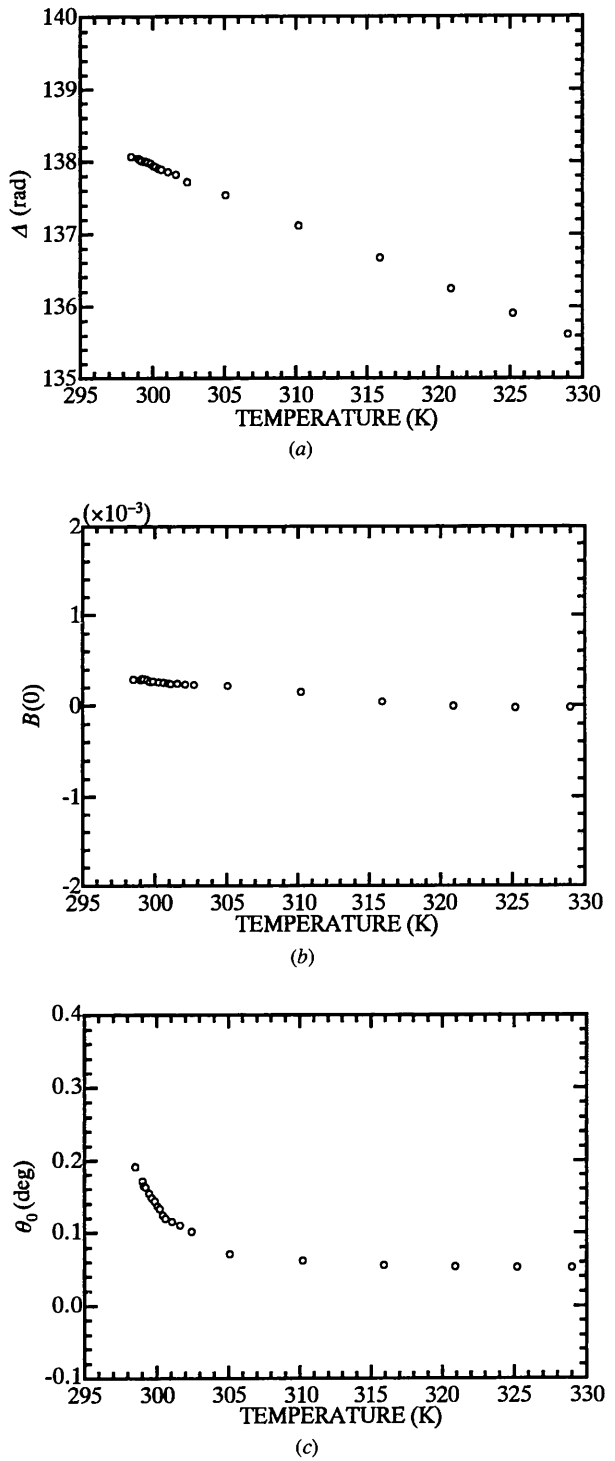

Fig. 3. Temperature dependences of (*a*) Δ, (*b*) $B(0)$ and (*c*) θ_0 of $LiNbO_3$. The azimuth is referred to the optically fast (*c*) axis.

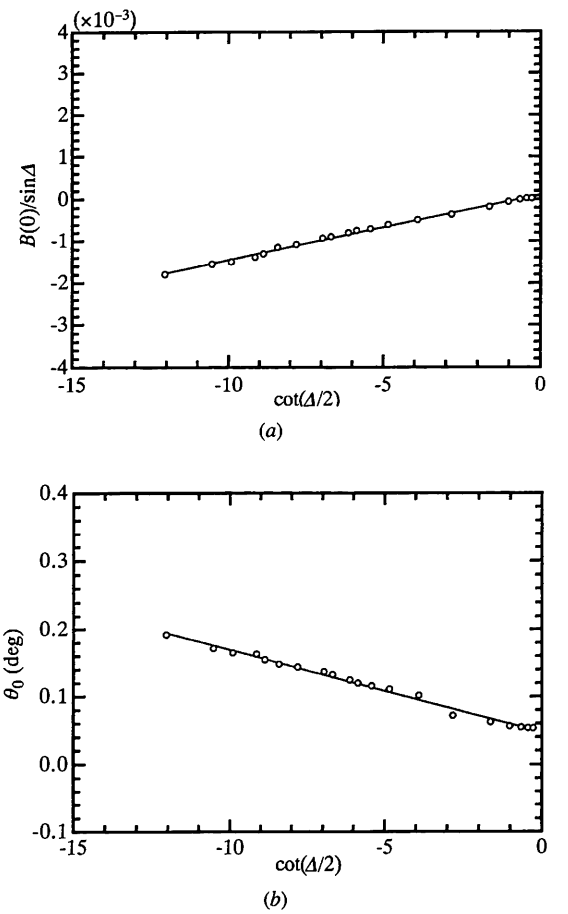

Fig. 4. Changes of (*a*) $B(0)/\sin\Delta$ and (*b*) θ_0 of $LiNbO_3$ with respect to $\cot(\Delta/2)$.

G and Δn could be readily deduced. The process of determination of systematic errors was described in detail in previous papers (Kobayashi & Uesu, 1983; Kobayashi, Kumomi & Saito, 1986; Kobayashi, Asahi, Takahashi & Glazer, 1988), so the analogous explanations in the present experiments are omitted except for specimens (ii) and (iv), where characteristic problems caused by the monoclinic symmetry were involved. However, an important remark must be made here on the application of the reference crystal method. We used $LiNbO_3$ (point group C_{3v}) as the reference crystal. To deduce the systematic error p, k in (4) or (5) was assumed to vanish, since the crystal is centrosymmetric. Simon, Weber & Unruh (1996) insist from the result of their HAUP measurements that a centrosymmetric MgF_2 crystal manifested non-zero k probably through surface treatments like polishing. Although this

Table 1. *Dimensions and systematic errors of the specimens used in the present experiment*

Specimen	Area (mm × mm)	Thickness (mm)	p ($\times10^{-4}$)	q ($\times10^{-4}$)	γ ($\times10^{-4}$)	$\delta\Upsilon$ ($\times10^{-4}$)
(i)	2.32 × 1.65	0.104	2.3	−1.8	4.1	1.2
(ii)	1.13 × 0.51	0.371	5.7	22.1	−16.4	7.7
(iii)	0.64 × 0.29	0.109	5.0	−9.3	14.3	−9.4
(iv)	0.72 × 0.42	0.166	2.4	−8.8	11.2	1.9

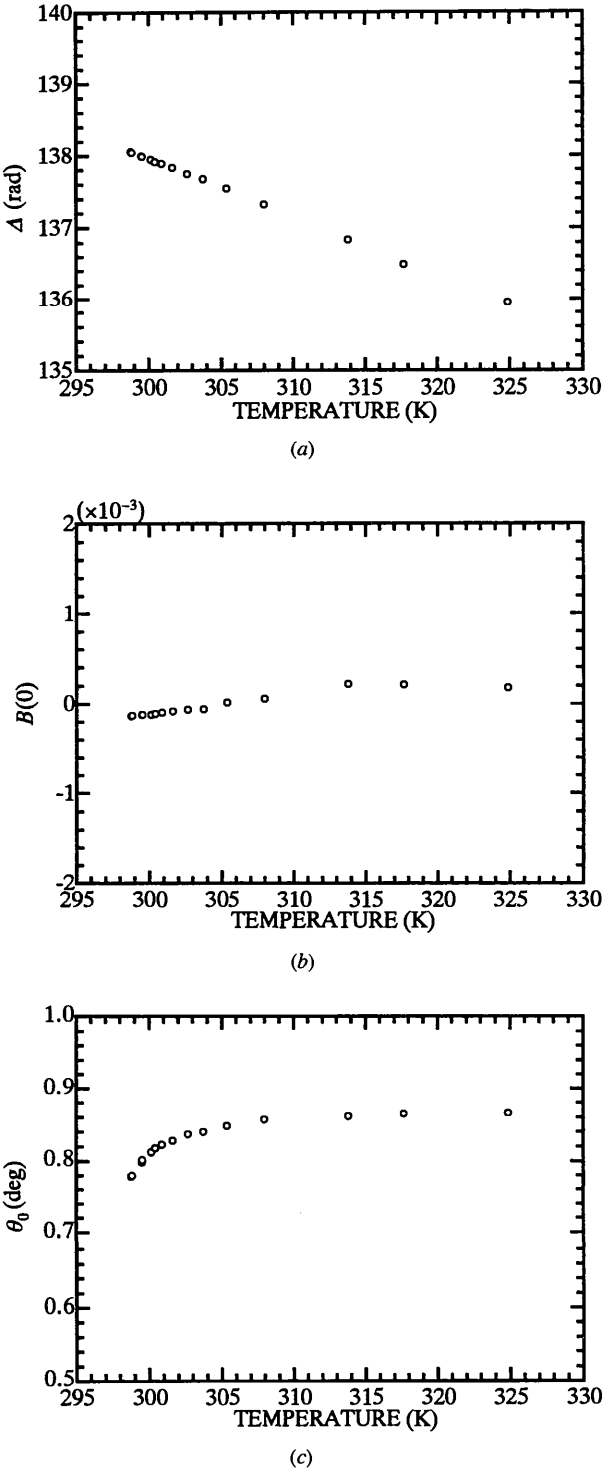

Fig. 5. Temperature dependences of (*a*) Δ, (*b*) $B(0)$ and (*c*) θ_0 of $LiNbO_3$. The azimuth is referred to the optically slow (b^*) axis.

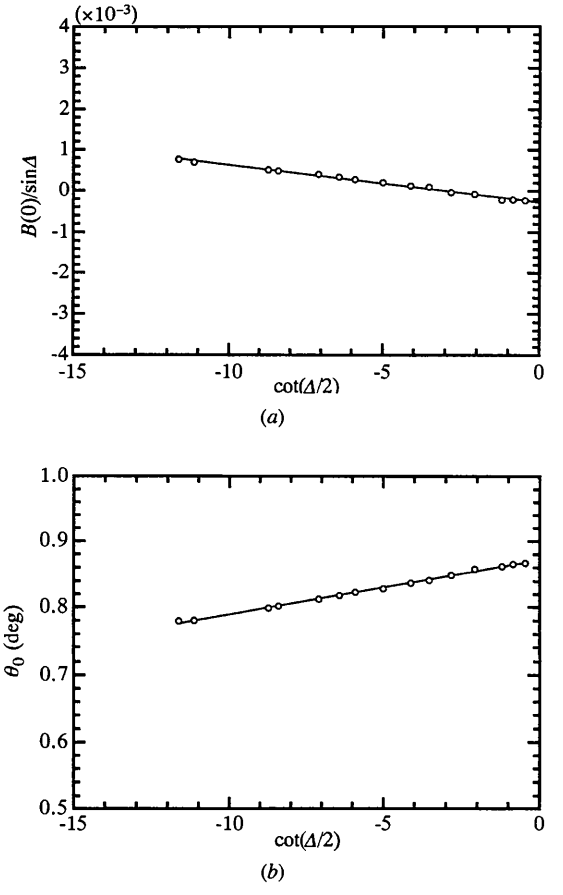

Fig. 6. Changes of (*a*) $B(0)/\sin\Delta$ and (*b*) θ_0 of $LiNbO_3$ with respect to $\cot(\Delta/2)$.

phenomenon seemed unlikely from our experiences using carefully prepared specimens, we felt it necessary to demonstrate the vanishing of k in our $LiNbO_3$ crystals experimentally.

A (100) specimen of $LiNbO_3$ with area 1.505×3.552 mm and thickness 0.166 mm was prepared, where the smooth surfaces were obtained by using Al_2O_3 abrasive of 0.3 μm. The azimuth was

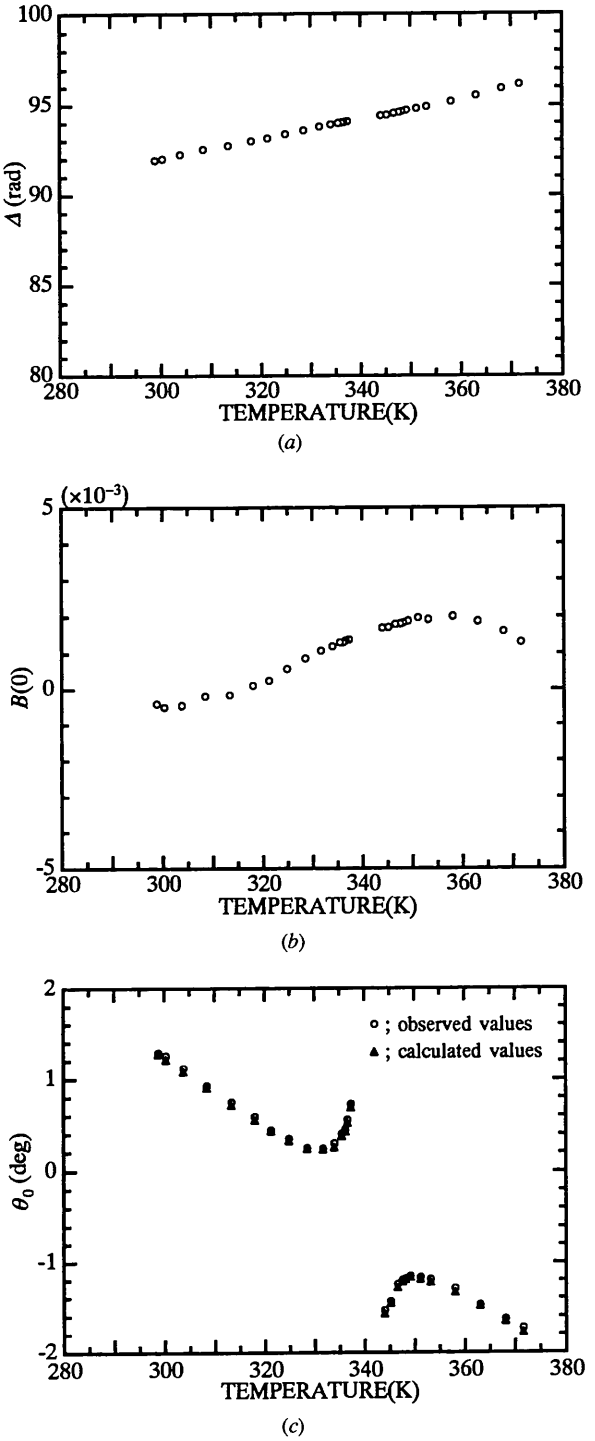

Fig. 7. Temperature dependences of (*a*) Δ, (*b*) $B(0)$ and (*c*) θ_0 of specimen (ii) of L-AA. In (*c*), the calculated values of θ_0 are indicated by the solid triangles.

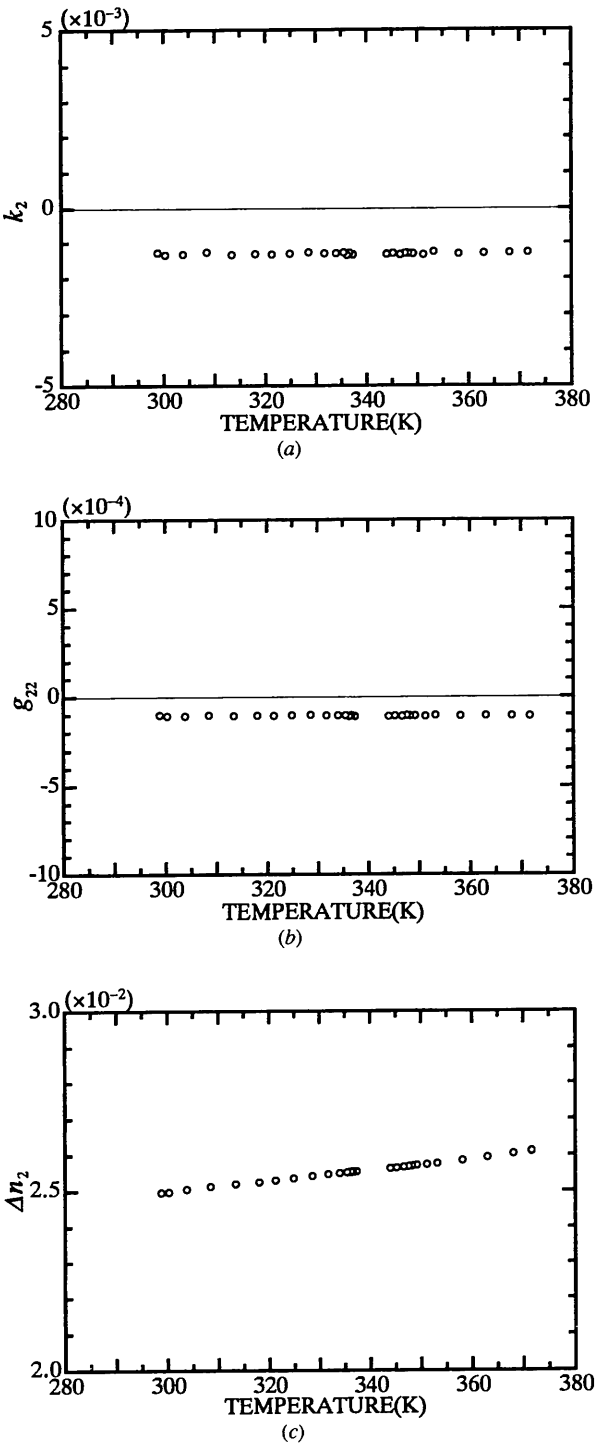

Fig. 8. Temperature dependences of (*a*) k_2, (*b*) g_{22} and (*c*) Δn_2 of specimen (ii) of L-AA.

referred to the optically fast axis (c axis) first. Temperature dependences of Δ, $B(0)$ and θ_0 are represented in Figs. 3(a), (b) and (c), respectively. From these figures, $B(0)/\sin\Delta$ and θ_0 could be expressed as a function of $\cot(\Delta/2)$, as shown in Figs. 4(a) and (b). Perfectly linear curves were found in both figures, showing that k was strictly independent of temperature. From the intercept and the derivative of the $B(0)/\sin\Delta$ line, $p-q-2k=1.12(17)\times10^{-4}$ and $\delta\Upsilon=1.56(2)\times10^{-4}$, respectively. From the derivative of θ_0, $p+q=4.19(9)\times10^{-4}$. Thus, $p-k$ was found to be $2.66(13)\times10^{-4}$.

When the specimen rotated by 90° around the a axis, $B(0)$ and θ_0 changed to $B'(0)$ and θ'_0. It is clear that k and Δ changed their signs in this case. As the incident condition of light on the polarizer was not altered, p should remain unchanged in the new system. However, q and $\delta\Upsilon$ might be changed to q' and $\delta\Upsilon'$. Then, (5) and (6) become in this system

$$B'(0)/\sin\Delta=-p+q'-2k+\delta\Upsilon'\cot(\Delta/2) \quad (7)$$

and

$$\theta'_0=\tfrac{1}{2}(p+q')\cot(\Delta/2)-\tfrac{1}{2}\delta\Upsilon'. \quad (8)$$

Temperature dependences of Δ, $B'(0)$ and θ'_0 are shown in Figs. 5(a), (b) and (c). $B'(0)/\sin\Delta$ and θ'_0 are depicted in Figs. 6(a) and (b) with respect to $\cot(\Delta/2)$, where perfect linear relations hold again. From Fig. 6(a), $-p+q'-2k=-2.74(15)\times10^{-4}$ and $\delta\Upsilon'=-9.1(2)\times10^{-5}$. It is seen that $\delta\Upsilon$ and $\delta\Upsilon'$ are different as anticipated. From Fig. 6(b), $p+q'=2.87(4)\times10^{-4}$. Therefore, $p+k$ was evaluated to be $2.81(10)\times10^{-4}$. By using the previous value of $p-k$, the following results were derived: $k=0.8(12)\times10^{-5}$, $p=2.74(12)\times10^{-4}$, $q=1.45(21)\times10^{-4}$ and $q'=1.3(16)\times10^{-5}$. Thus, it was verified that k could be regarded to disappear within the accuracy of the present measurements. Also, q was different from q' as expected. The systematic errors of the four specimens obtained by using this method are shown in Table 1, together with the dimensions. It may be noted that the systematic errors alter according to changes of incident conditions of light on the polarizer and analyzer (Kobayashi, Kumomi & Saito, 1986; Kobayashi, Asahi, Takahashi & Glazer, 1988).

In order to determine temperature dependences of G_2 and Δn_2 of specimen (ii), Ψ was provisionally expanded as a power series of T,

$$\Psi=B_0+B_1T+B_2T^2. \quad (9)$$

Then, (6) becomes

$$\theta_0=-\tfrac{1}{2}(p+q)\cot(\Delta/2)+B_1T+B_2T^2+C, \quad (10)$$

where C designates a constant which depends on the reading system of the azimuth (Kobayashi & Uesu, 1983). Temperature dependences of Δ, $B(0)$ and θ_0 are shown in Figs. 7(a), (b) and (c) as open circles. From Figs. 7(a) and (c), the numerical relationship between θ_0 and Δ was obtained. Then it was possible to determine $p+q$, B_1, B_2 and C, which fitted the above relationship, by the least-squares method; the results being $p+q=2.78\times10^{-3}$, $B_1=-6.98\times10^{-4}$, $B_2=4\times10^{-7}$ and $C=4.088\times10^{-2}$. The calculated values of θ_0 by using these parameters are plotted in Fig. 7(c) as solid triangles, showing good coincidence with the observed values. The temperature derivative of Ψ, $d\Psi/dT$, was $-4.3\times10^{-2}\,K^{-1}$. As p had already been determined by the reference crystal method, temperature dependences of k_2, g_{22} and Δn_2 were acquired as shown in Figs. 8(a), (b) and (c).

The incident angle θ in (2) between s and the x_3 axis in specimen (iv) was determined using the Weissenberg method. We took a Weissenberg photograph of the specimen around the b axis, when the position of normal incidence of X-rays on the specimen was marked by a spot exposure on the ω coordinate of the film. Then, the angle was calculated from the distances between the spot and (h00) or (00l) lines. By using g_{11} and g_{33}

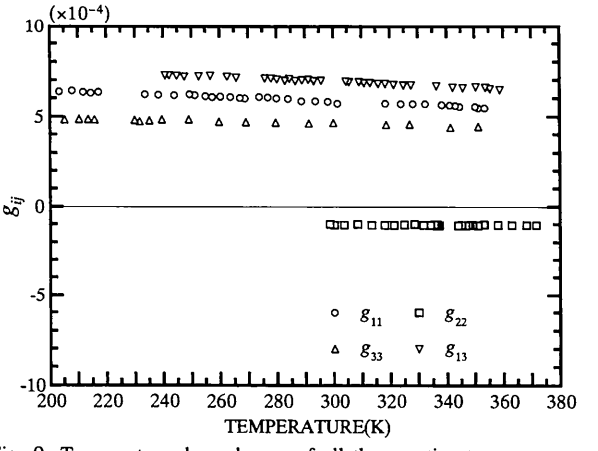

Fig. 9. Temperature dependences of all the gyration-tensor components g_{ij} of L-AA.

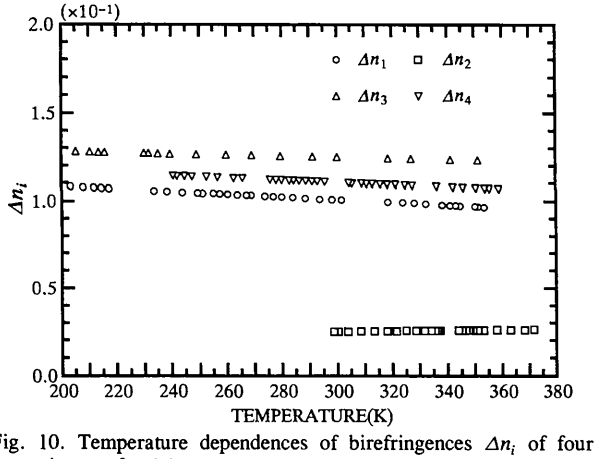

Fig. 10. Temperature dependences of birefringences Δn_i of four specimens of L-AA.

determined from specimens (i) and (iii), g_{13} was calculated from (2).

Temperature dependences of all the components of the gyration tensor and the birefringence of L-AA are indicated in Figs. 9 and 10, respectively. The gyration-tensor components at room temperature were $g_{11} = 5.84 \times 10^{-4}$, $g_{22} = -1.02 \times 10^{-4}$, $g_{33} = 4.72 \times 10^{-4}$ and $g_{13} = 6.95 \times 10^{-4}$. Birefringences at the same temperature were $\Delta n_1 = 1.01 \times 10^{-1}$, $\Delta n_2 = 2.5 \times 10^{-2}$, $\Delta n_3 = 1.27 \times 10^{-1}$ and $\Delta n_4 = 1.10 \times 10^{-1}$.

4. Discussion

Here the gyration surface (Shubnikov, 1960) and chirality index (Asahi, Utsumi, Itagaki, Kagomiya & Kobayashi, 1996) of L-AA are discussed. The equation of the three-dimensional gyration surface of the crystal is given as

$$G = g_{11}\cos^2\theta_1 + g_{22}\cos^2\theta_2 + g_{33}\cos^2\theta_3 + 2g_{13}\cos\theta_1\cos\theta_3. \quad (11)$$

Therefore, the equation of the intersection of the gyration surface with the (x_1, x_2) plane, *viz* the gyration figure, becomes

$$G = g_{11}\cos^2\theta_1 + g_{22}\cos^2\theta_2. \quad (12)$$

This figure is schematically depicted in Fig. 11(*a*), where white and black ovoids designate the positive and negative gyrations, respectively. The directions of $G = 0$ in this plane are given by $\theta_1 = \tan^{-1}[\pm(-g_{11}/g_{22})^{1/2}] = \pm 67.3°$, by equating (12) to zero. Similarly, the gyration figure on the (x_2, x_3) plane is shown in Fig. 11(*b*) and the directions of $G = 0$ are given by $\theta_2 = \pm 24.9°$. The equation of the gyration figure on the (x_3, x_1) plane is

$$G = g_{11}\sin^2\theta_3 + g_{33}\cos^2\theta_3 + 2g_{13}\sin\theta_3\cos\theta_3. \quad (13)$$

Thus, it is seen that the principal axes of the gyration figure rotate around the x_2 axis. Equation (13) changes to

$$G = (g_{11}+g_{33})/2 + [g_{13}^2 - (g_{33}-g_{11})^2/4]^{1/2}\sin(2\theta_3 + \alpha), \quad (14)$$

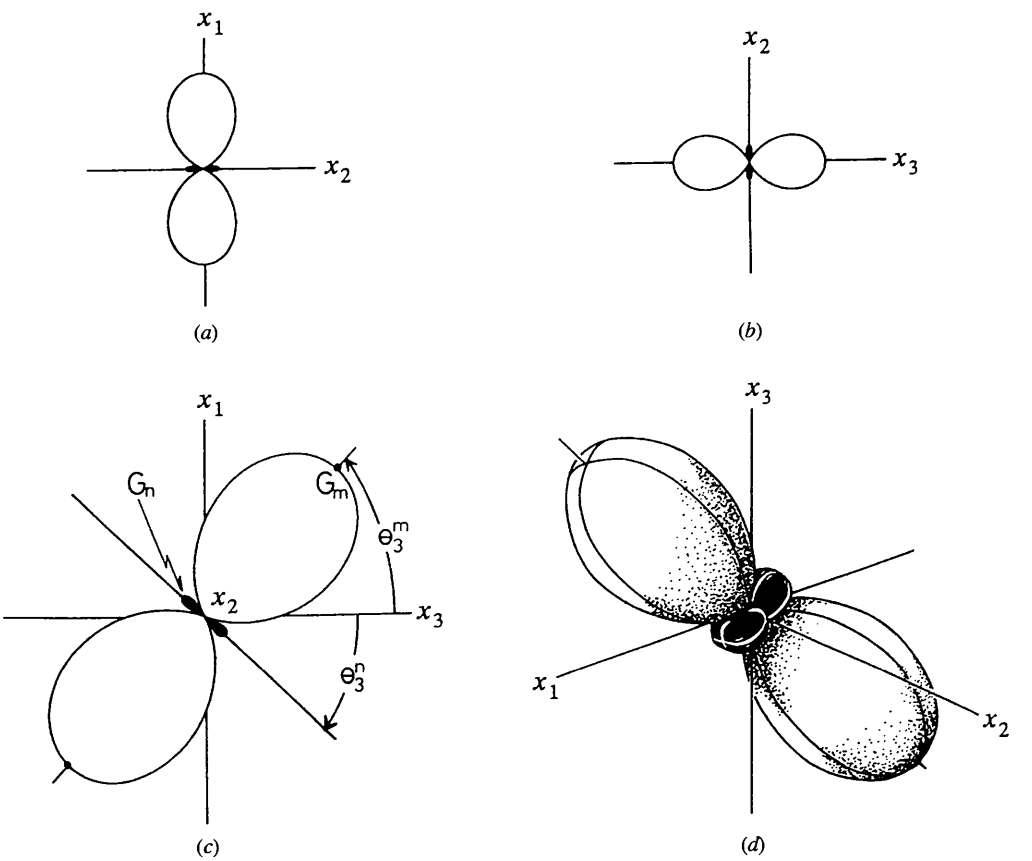

Fig. 11. Schematic representations of the gyration surface of L-AA. (*a*) The gyration figure on the (x_1, x_2) plane; (*b*) the gyration figure on the (x_2, x_3) plane; (*c*) the gyration figure on the (x_3, x_1) plane, where the principal axes of the gyration figure are indicated. (*d*) Perspective view of the gyration surface.

where

$$\alpha = \tan^{-1}[(g_{33} - g_{11})/2g_{13}]. \quad (15)$$

Define the direction of θ_3 showing G_m, the maximum G value, as θ_3^m. It is determined by the condition of $\sin(2\theta_3^m + \alpha) = 1$. Similarly, the minimum direction θ_3^n showing the minimum G_n is given by $\sin(2\theta_3^n + \alpha) = -1$. These are expressed as

$$\theta_3^m = \tfrac{1}{2}(\pi/2 - \alpha) \quad \text{and} \quad \theta_3^n = \tfrac{1}{2}(\pi/2 + \alpha). \quad (16)$$

Further,

$$G_m = (g_{11} + g_{33})/2 + [g_{13}^2 - (g_{33} - g_{11})^2/4]^{1/2}$$

and

$$G_n = (g_{11} + g_{33})/2 - [g_{13}^2 - (g_{33} - g_{11})^2/4]^{1/2}. \quad (17)$$

The gyration figure on the (x_3, x_1) plane is shown in Fig. 11(*c*). The directions of $G = 0$ are given by $\theta_3 = -22.3$ and $-63.1°$. Examples of G_m and G_n values are as follows: $G_m = 1.225 \times 10^{-3}$ $(2.234 \times 10^{3\circ}\,\mathrm{cm}^{-1})$ at $\theta_3^m = 47.3°$ and $G_n = -1.69 \times 10^{-4}$ $(-3.08 \times 10^{2\circ}\,\mathrm{cm}^{-1})$ at $\theta_3^n = -42.7°$, where corresponding rotatory powers are indicated in parentheses. From (16), the temperature dependence of θ_3^m could be obtained as depicted in Fig. 12. The temperature derivative, $\mathrm{d}\theta_3^m/\mathrm{d}T$, is evaluated as $-5.5 \times 10^{-3\circ}\,\mathrm{K}^{-1}$. It is approximately 1/8 of $\mathrm{d}\Psi/\mathrm{d}T$. A perspective view of the gyration surface is depicted in Fig. 11(*d*), where the dimension of the black oblong 'boublik' (Shubnikov, 1960) is exaggeratedly drawn.

Let us calculate the chirality index, which was defined by Asahi, Utsumi, Itagaki, Kagomiya & Kobayashi (1996). The averaged gyration tensor of the crystal, $\bar{g}$, is given by G_m, G_n and g_{22},

$$\bar{g} = \tfrac{1}{3}(G_m + G_n + g_{22}) = 3.18 \times 10^{-4}. \quad (18)$$

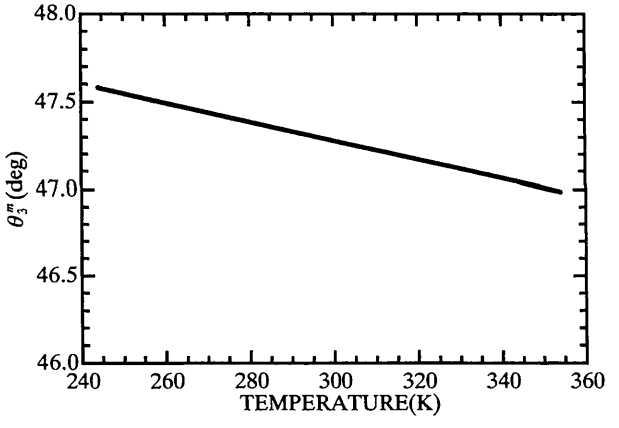

Fig. 12. Temperature dependence of θ_3^m, the direction of θ_3 showing maximum G.

Then the rotatory power of the crystal aggregate of the unit volume, containing randomly oriented crystallites, is expressed as

$$\rho_c = 180\bar{g}/\lambda\bar{n} = 5.80 \times 10^2\,[^\circ\,\mathrm{cm}^{-1}\,\mathrm{ml}^{-1}], \quad (19)$$

where $\bar{n} = 1.56$ (Delfino, 1979) is the mean refractive index. On the other hand, the number of AA molecules contained in the unit volume is $N_c = Z/abc\sin\beta = 7.37 \times 10^{21}\,\mathrm{cm}^{-3}$, where $Z = 2$ is the number of molecules contained in a unit cell. Therefore, the rotatory power per molecule in the crystalline state is given by

$$\rho_c^0 = \rho_c/N_c = 7.87 \times 10^{-20}\,[^\circ\,\mathrm{cm}^{-1}]. \quad (20)$$

Katzin & Gulyas (1964) measured the specific rotation $[\alpha] = 21.5^\circ\,\mathrm{dm}^{-1}\,(\mathrm{g\,ml}^{-1})^{-1}$ in the solvent 2*M* HCl. Then, the molecular rotation $[M]$ becomes $(M/100)[\alpha] = 28.6^\circ\,\mathrm{dm}^{-1}\,(\mathrm{mol\,100\,ml}^{-1})^{-1}$. So the rotatory power ρ_s^0 of a molecule in the solution is

$$\rho_s^0 = 10[M]/N_A = 4.75 \times 10^{-22}\,[^\circ\,\mathrm{cm}^{-1}], \quad (21)$$

where N_A designates Avogadro's number. Thus, the chirality index of L-AA is obtained as

$$r = (\rho_c^0 - \rho_s^0)/\rho_c^0 = 0.994. \quad (22)$$

This value is a measure of the crystal-structure contribution of the crystal to the OA and represents the severity of the restriction of the freedom of molecular orientation by forming a crystal lattice. We have already derived $r = 0.992$ for glutamic acid. It is of special interest that the r values of the two amino acids are almost the same. It will be useful to study r values for other amino acids.

The authors thank Mr H. Utsumi and Mr Y. Itagaki for their helpful contributions to this work.

References

Asahi, T., Utsumi, H., Itagaki, Y., Kagomiya, I. & Kobayashi, J. (1996). *Acta Cryst.* A**52**, 766–769.
Bernal, J. D. (1931). *Z. Kristallogr.* **78**, 363-369.
Delfino, M. (1979). *Mol. Cryst. Liq. Cryst.* **52**, 271–284.
Derissen, J. L., Endeman, H. J. & Peerdeman, A. F. (1968). *Acta Cryst.* B**24**, 1349–1354.
Fujii, N., Ishibashi, Y., Satoh, K., Fujino, M. & Harada, K. (1994). *Biochim. Biophys. Acta*, **1204**, 157–163.
Fujii, N., Satoh, K., Harada, K. & Ishibashi, Y. (1994). *J. Biochem.* **116**, 663–669.
Katzin, L. I. & Gulyas, E. (1964). *J. Am. Chem. Soc.* **86**, 1655–1659.
Kobayashi, J., Asahi, T., Takahashi, S. & Glazer, A. M. (1988). *J. Appl. Cryst.* **21**, 479–484.
Kobayashi, J., Kumomi, H. & Saito, K. (1986). *J. Appl. Cryst.* **19**, 377–381.
Kobayashi, J. & Uesu, Y. (1983). *J. Appl. Cryst.* **16**, 204–211.
Masters, P. M., Bada, J. L. & Zigler, J. S. Jr (1977). *Nature (London)*, **268**, 71–73.

Moxon, J. R. L. & Renshaw, A. R. (1990). *J. Phys. Condens. Matter*, **2**, 6807–6836.
Shubnikov, A. V. (1960). *Principles of Optical Crystallography*, p. 128. New York: Consultants Bureau.
Simon, J., Weber, J. & Unruh, H.-G. (1996). *Ferroelectrics*, **183**, 161–170.
Suresh, C. G. & Vijayan, M. (1983). *Int. J. Pept. Protein Res.* **22**, 176–178.